



ELSEVIER

Applied Surface Science 168 (2000) 345–352

applied  
surface science

www.elsevier.nl/locate/apsusc

# Direct writing of conformal mesoscopic electronic devices by MAPLE DW

D.B. Chrisey<sup>\*</sup>, A. Pique, R. Modi, H.D. Wu,  
R.C.Y. Auyeung, H.D. Young

*Naval Research Laboratory, Plasma Processing Section, Code 6372, Washington, DC 20375-5345, USA*

## Abstract

We demonstrate a novel pulsed UV laser direct writing technique called MAPLE DW for the fabrication of conformal electronic devices. MAPLE DW (matrix assisted pulsed laser evaporation direct write) is a soft laser forward transfer technique that takes place in air and at room temperature. Specific experimental results for the deposition of Ag metal and BaTiO<sub>3</sub> composite dielectrics with electrical quality comparable to conventional thick film deposition techniques will be given as well as a discussion of the relevant issues for further electronic device improvement. The mechanism of the MAPLE DW process that makes it applicable to a broad class of electronic materials and even biomaterials is also described. Published by Elsevier Science B.V.

*Keywords:* Thin films; Electronic devices; Laser deposition; Direct writing; Matrix assisted pulsed laser evaporation direct write (MAPLE DW)

## 1. Introduction

There is a strong need in the electronics industry to reduce product design and development times and to adaptively produce small lots at a competitive cost. Conventional thick film techniques like screen printing and low resolution lithography require several iterations of the development cycle: circuit design, mask fabrication, prototype manufacture, testing and evaluation before a new electronic device or subsystem can go to market. Rapid prototyping techniques do exist, but their function is to produce something that has morphological similarities to the desired final product. Almost without exception, existing rapid

prototyping techniques do not work with electronic materials much less a wide range of electronic materials (conductors, dielectrics, resistors, etc.) and with CAD/CAM capability. Mesoscopic direct write techniques are not intended to compete with current photolithographic circuit design and fabrication approaches, but instead direct write techniques that work seamlessly with different materials will enable new design and manufacturing capabilities.

MAPLE DW (matrix assisted pulsed laser evaporation direct write) is a relatively new technique that can satisfy the industrial need to do rapid prototyping of a wide range of different electronic materials [1–3]. In Fig. 1a, we present a schematic diagram of the MAPLE DW system and in Fig. 1b, we illustrate how each laser pulse deposits a highly reproducible “brick” of electronic material. When successful laser pulses are placed in specific locations and the bricks

<sup>\*</sup> Corresponding author. Tel.: +1-202-767-4788;  
fax: +1-202-767-5301.  
E-mail address: chrisey@ccf.nrl.navy.mil (D.B. Chrisey).

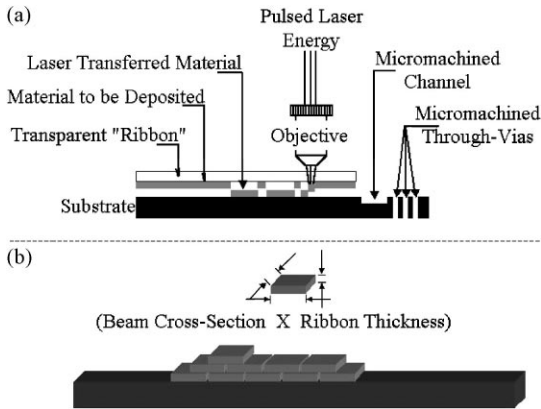


Fig. 1. (a) Schematic diagram of the MAPLE DW system and (b) an illustration of how individual laser pulses are combined to form electronic circuit elements.

of electronic material add to form an electronic circuit element and subsequently, when individual elements are combined, electronic subsystems.

MAPLE DW is a laser forward transfer technique similar in experimental approach to laser induced forward transfer (LIFT) [4–10]. The difference between the two techniques, which therein lies the novelty of the MAPLE DW, is the interaction of the laser with the ribbon coating. In LIFT, the laser ablates or vaporizes the dense coating into atoms, ions and small molecules, whereas in MAPLE DW the laser softly transfers a coating of micron size powders, nanoparticles, chemical precursors and various minor additives. The two techniques are similar in that by removing the coated ribbon the deposition system has all the attributes of a conventional laser micromachining system. This allows in situ laser surface pre-treatment, surface annealing and circuit element trimming. Other advantages of MAPLE DW include high-resolution ( $2\ \mu\text{m}$ ) patterns, high write speeds ( $>200\ \text{mm/s}$ ), the ability to transfer a wide variety of materials (ceramics, metals, ferrites, polymers), CAD/CAM rapid prototyping, high-reproducibility, all in a dry process that is environmentally safe.

The novelty in the MAPLE DW process is in the soft transfer of a composite material made up of micron-size powders, nanoparticles and chemical precursors. The composite material transfers and forms a mechanically dense packing. The theoretical packing of spherical powders is 74% for the face-centered

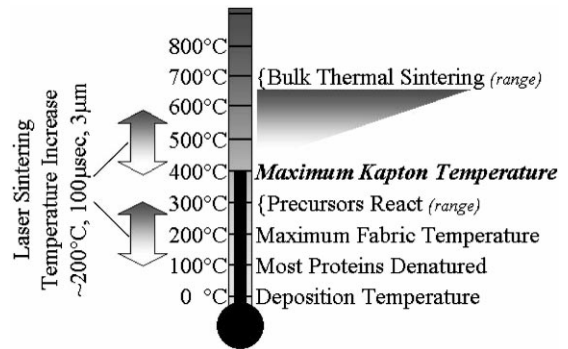


Fig. 2. A temperature scale providing the typical temperatures or temperature ranges for physical processes associated with direct writing of electronic materials.

cubic packing structure. With the addition of nanoparticles to fill the interstitial voids, this value should increase. An additional novelty in the MAPLE DW process is in the use of low decomposition temperature chemical precursors. Fig. 2 illustrates a temperature scale of useful temperatures and temperature ranges for direct write processes, for maximum polymer substrate temperatures and for bulk sintering. Even when chemical precursors react at temperatures low enough to allow the use of polymer substrates like Kapton, additional thermal processing will improve electronic properties. One way to overcome this liability is through the use of laser surface sintering.

In laser surface sintering, a pulsed laser interacts with the coating to a depth given by the laser penetration depth. Absorption of this radiation will thermally process the surface of the coating to a depth that is slightly larger depending on the thermal properties of the underlying material. The combination of thermal sintering, to temperatures below the threshold for substrate degradation and laser surface sintering will allow some of the benefits of bulk thermal sintering to be realized. In Fig. 3, we provide a schematic diagram of laser surface sintering combined with the MAPLE DW process. Through the use of special dichroic optics, both the UV transfer pulse and a specially chosen IR pulse, typically with wavelengths between 1 and  $10\ \mu\text{m}$ , can use the same alignment and transfer beam path. Ideally, the specific IR wavelength is chosen based on the maximum optical absorption of the deposited material, i.e., it is crucial to avoid laser heating of the substrate. In general, the optimized adsorption wavelengths of conductors are closer to

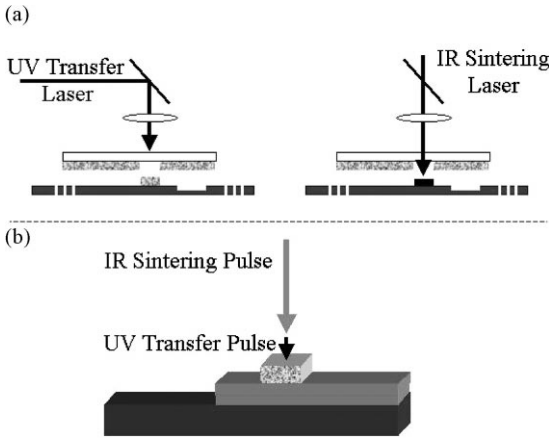


Fig. 3. A schematic diagram of laser surface sintering combined with the MAPLE DW transfer process. This combination will allow the benefits of bulk thermal sintering to be realized on polymer substrates.

1  $\mu\text{m}$ , whereas dielectrics are closer to 10  $\mu\text{m}$ . Similarly, the beam pulse width must be chosen for optimum thermal processing without degradation to the substrate. On the left side of the scale in Fig. 2 an approximation of the thermal benefits of laser surface sintering is given, i.e., approximately 200°C temperature increase for 100 ms and to a depth of 3  $\mu\text{m}$ . Loosely, this temperature increase allows the use of chemical precursors on biological substrates and for some measure of bulk sintering to take place on polymer substrates.

The goal of the MAPLE DW process is to produce a CAD/CAM direct written coating at low temperatures with electronic properties comparable to conventional thick film techniques. In order for this to occur, a dense coating of crystalline material must precede the reaction of the chemical precursors. A composite coating of micron-size powders combined with nanopowders

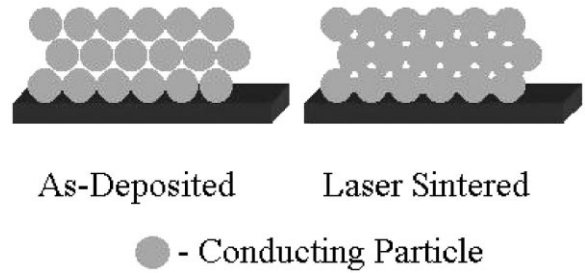


Fig. 4. The deposition and laser sintered bonding of powders, nanopowders and chemical precursors.

to fill the interstitial voids and chemical precursors is the ideal starting point. Then, the reaction of the chemical precursors, either by thermal processing alone or with the combination of laser surface sintering, should provide the chemical welding of the composite coating together. In Fig. 4, a schematic diagram of this ideal process is given. As shown in this figure, the bonding of the crystalline powder material to its nearest neighbors, either by reacting the chemical precursors or by the bulk diffusion in the nanopowders, yields a densified and adherent coating with superior electronic properties.

The issue of densification applies to all discrete circuit elements. As shown in Table 1, the electronic device issues for densification are profound, especially for the dielectrics. In porous dielectrics, the air that fills the interstitial voids dominates the effective dielectric constant. For the metal and ceramic materials, the issue of discrete circuit performance and densification is typically addressed through high temperature annealing. Conventional thick film techniques are, thus, only applicable to ceramic substrates which can withstand the required high temperature processing. To obtain the highest possible performance at the lowest possible temperatures, it is inher-

Table 1  
Densification issues for MAPLE DW of discrete electronic components

Passive component	Laser sintering, microstructure	Device issues
Metallic conductor	Intermediate mp, necking, porosity	Microwave surface resistance, power loss
Dielectric (ceramic oxides)	High mp, difficult to neck particles, oxygen loss	Porous material has drastic effect on $k$ , loss
Resistor (ceramic/insulator)	High mp, most difficult to neck around insulator	Conductor/insulator composite
Resistor (polymer/insulator)	Low processing temperature, necking around insulator	Aging, electromigration
Ceramic ferrite	High mp, difficult to neck particles, oxygen loss	Porous material has drastic effect on $\mu$ , loss, high $H_c$

ent that the MAPLE DW process start with a dense powder, nanopowders and chemical precursor composite.

## 2. Results

MAPLE DW, like all laser-material interactions, depends on both laser and material properties for optimized performance. In Fig. 5a, we give the optical micrographs for the material transferred by a  $30\ \mu\text{m}$  circular laser spot on a ribbon of two different dielectric material compositions as a function of laser fluence and in Fig. 5b, we give the effect of fluence on the fabrication of a dielectric coating on an interdigitated capacitor. In Fig. 5a, the difference between composition A and B is dominated by the percentage of solvent used in the starting ribbon paste with former being higher. We see that for Fig. 5a and composition A, at low fluences the spot mimics the incident laser pulse and gradually becomes larger. At increasingly larger fluences, the uniformity of the perimeter of the

deposition and the lateral debris increases, whereas for composition B, the transferred material is entirely debris with little resemblance to the incident pulse. Experiments like this are important when trying to determine laser and material parameters for narrow line widths with minimal debris. Lateral resolution and debris are not a problem when fabricating interdigitated capacitors. In this case, the coating is made up of a dense array of closely packed individual spots. From Fig. 5b, it is clear that the cumulative effect of fluence from individual transfer spots can have a dramatic and macroscopic effect on the final capacitor properties. The capacitor fabricated at  $2.6\ \text{J}/\text{cm}^2$  is completely cracked which will result in a lower capacitance.

For almost all discrete circuit elements, edge definition can have a profound effect on the resulting element's electrical performance. This is especially the case for high frequency conductors in microwave devices. While the dc conductivity may be comparable or better than conventional thick film techniques, the high frequency behavior, as defined by the microwave

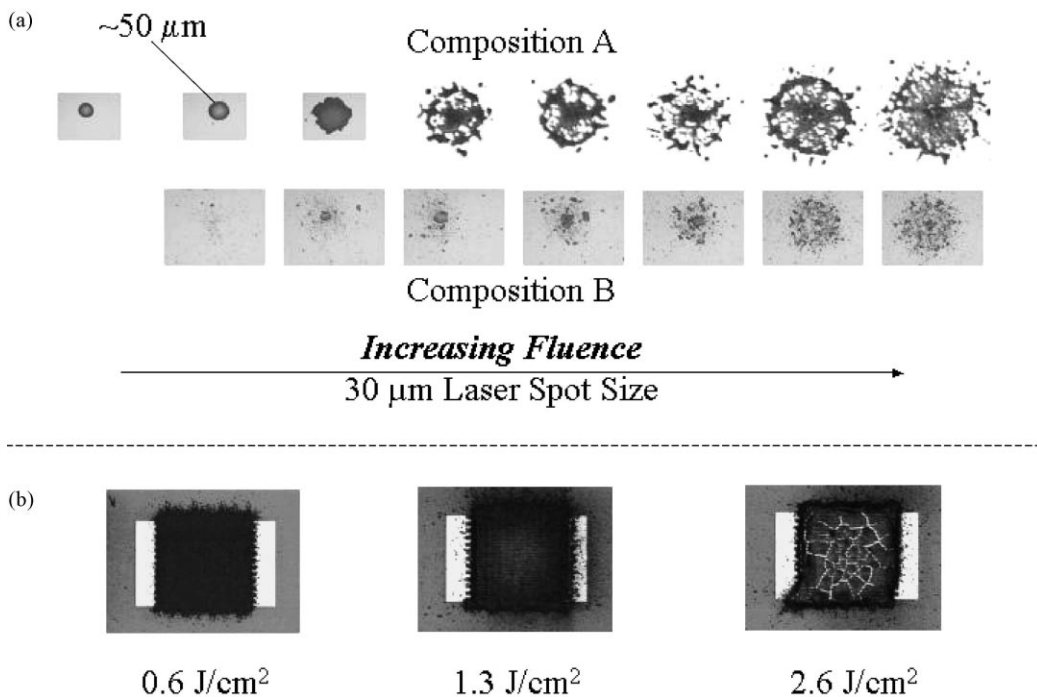


Fig. 5. (a) The deposition pattern for single laser transfer pulses is given vs. fluence and (b) the effect of fluence on the fabrication of a dielectric coating on an interdigitated capacitor is given.

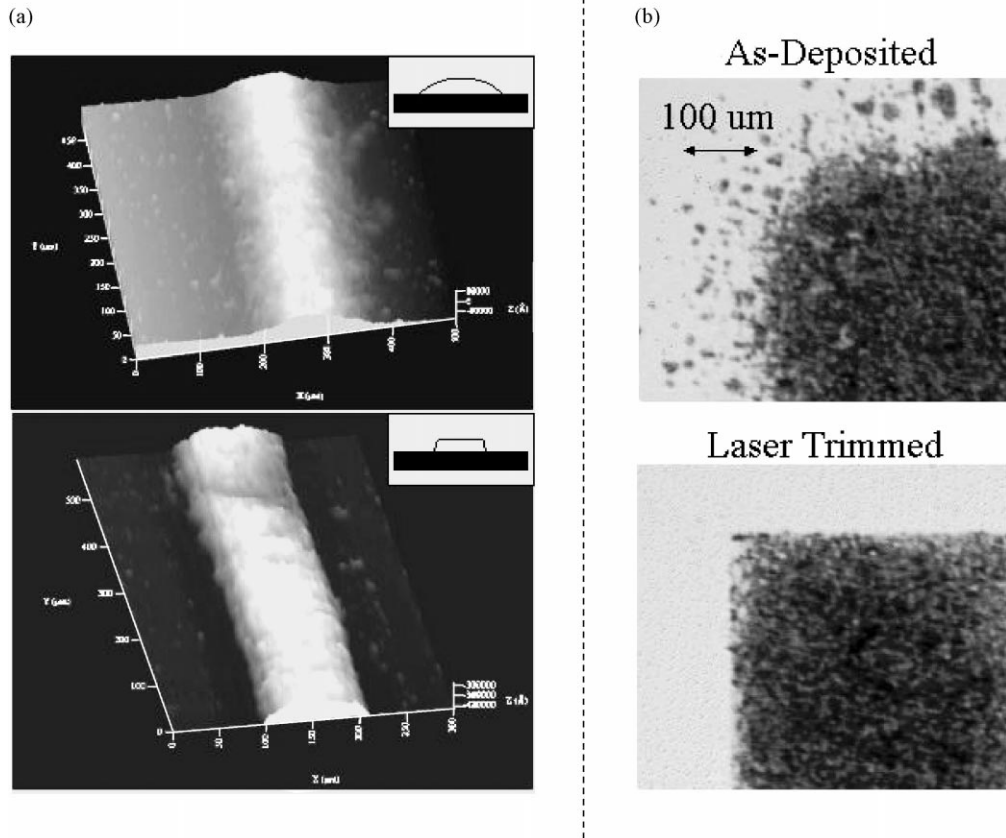


Fig. 6. The effect of in situ laser micro-machining to improve the morphology of discrete circuit elements: (a) the edge definition of a Ag conductor is improved by laser micro-machining the debris and (b) the lateral debris in a BaTiO<sub>3</sub> dielectric coating is removed to yield a sharp interface.

surface resistance ( $R_s$ ), may be very poor. This is because the higher frequencies impose specific spatial current distribution as compared to a percolating path observed at dc. In particular, at high frequencies (>1 GHz) the majority of the current is carried by the edges where debris and non-uniformities will dominate the overall  $R_s$ . One advantage of the MAPLE DW approach is the ability to do in situ laser micro-machining. In Fig. 6, we present optical micrographs of improvements made to a conductor and a dielectric coating that will improve the final circuit element performance.

In Fig. 7, we present an optical micrograph and contact profilometer scans at various lengths across a 8  $\mu\text{m}$  long by about 40  $\mu\text{m}$  FWHM wide Ag line fabricated by MAPLE DW. The uniformity of this

line is evidenced by the reproducibility of the cross scans at 1 mm increments along its length. The dc conductivity of this line is  $\sim 2.5$  times bulk Ag. This line was processed at temperatures below 300°C. Screen-printed Ag lines have conductivities between two and three times bulk Ag, but they are not CAD/CAM compatible, they cannot achieve line widths below  $\sim 100 \mu\text{m}$  and they cannot be deposited on temperature-sensitive polymer substrates. Conducting lines like that shown in Fig. 7 are made in a few seconds at a 10 Hz laser repetition rate and are used to optimize laser and material properties for discrete element performance. Analogously, the interdigitated capacitors of Fig. 5b are used to optimize the laser and materials for dielectric properties such as the dielectric constant and loss.

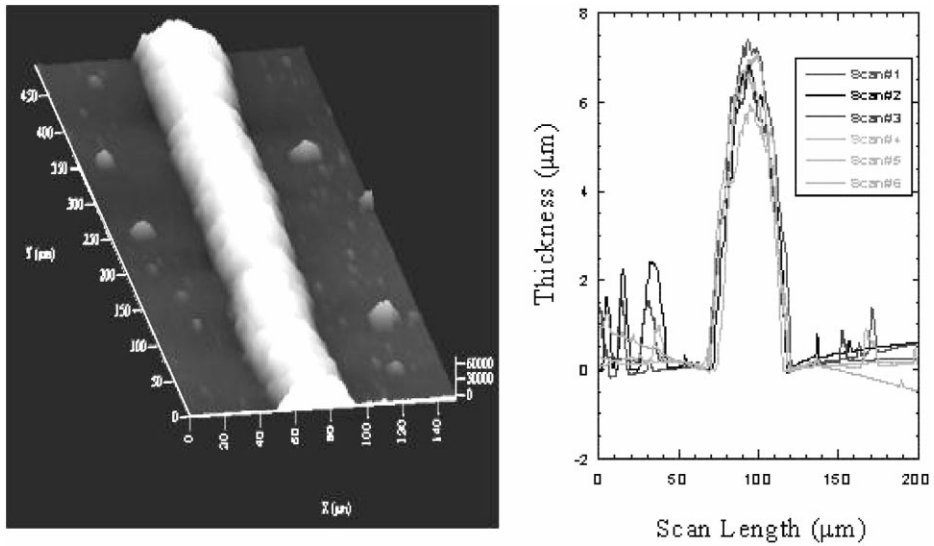


Fig. 7. Optical micrograph and contact profilometer scans of a MAPLE DW deposited Ag line. The dc conductivity of this line is  $\sim 2.5$  times bulk Ag and the FWHM line width is  $\sim 40 \mu\text{m}$ .

In Fig. 8, we present a summary of some of the discrete circuit elements fabricated by MAPLE DW. These circuit elements cover a wide range of electronic materials (conductors, dielectrics, phosphors), resolutions, as well as circuit patterns and multilevel circuit complexity. In particular, the YIG core inductor is a multi-turn Ag conductor around a planar YIG

core. Devices like these demonstrate that MAPLE DW can be used to create novel three-dimensional structures.

The value of examples of circuit elements like those given in Fig. 8 is motivation to develop aspects of the processing, but for ultimate industrial manufacturing to be realized, the electrical performance must be

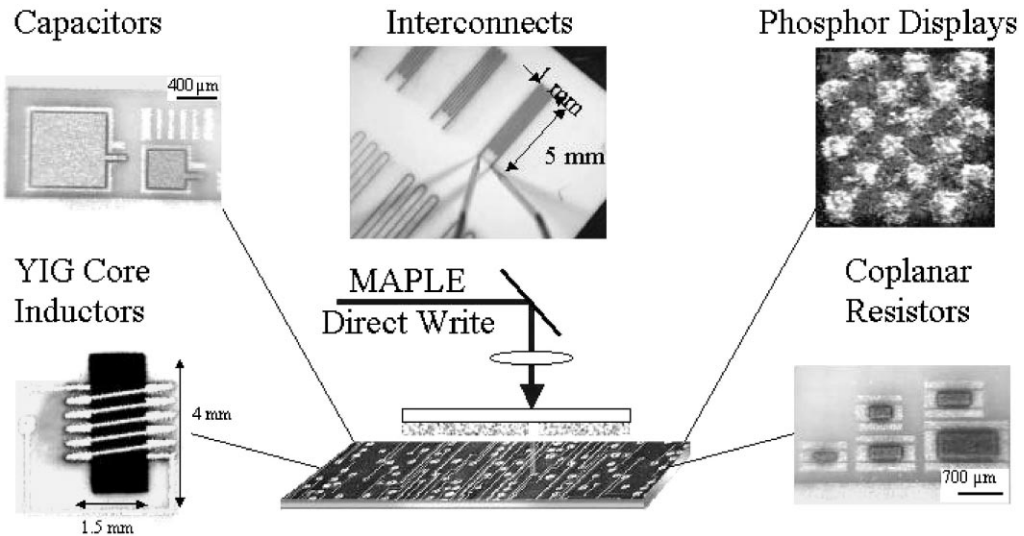


Fig. 8. A summary of some of the discrete circuit elements and materials fabricated using the MAPLE DW process.

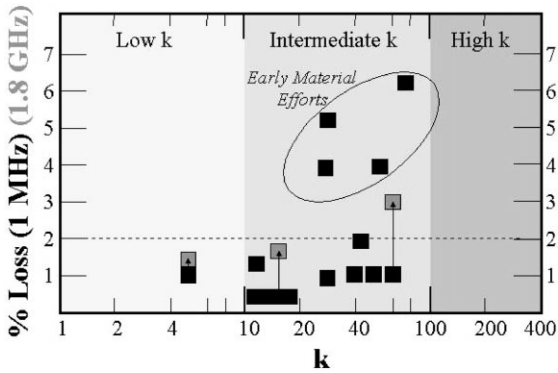


Fig. 9. The dielectric loss vs. the dielectric constant for MAPLE DW deposited dielectric materials. Also shown for comparison are the regions for low, intermediate and high  $k$  values and the value for 2% loss.

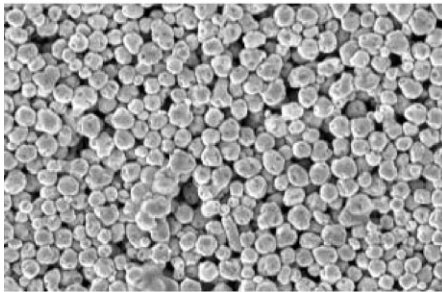
comparable to or better than existing technologies. The principal issue remaining for industrial insertion of the MAPLE DW process, besides development of the commercial tool, is the continued densification of the deposited composite. This is clear from the dielectric measurements. In Fig. 9, we present the dielectric loss at 1 MHz and 1.8 GHz versus the dielectric constant. In this plot we have indicated vertical regions for low  $k$  (1–10), intermediate  $k$  (10–100) and high  $k$  (100–400) as well as a horizontal dotted

line for 2% loss. While there are specific applications for the entire range in  $k$ , for storage applications, high  $k$  is preferable due to size constraints, i.e., the dielectric constant is inversely proportional to the size of the area needed for a parallel plate capacitor on a circuit subsystem, with all other parameters being kept equal. Another almost equally important parameter, which will not be covered here, is the thickness with which the dielectric layer can be deposited, i.e., the capacitance is inversely proportional to the electrode separation. Also, for almost all applications the dielectric loss must be less than 1%. For some applications like high quality factor devices, the loss must be even lower, e.g., 0.1%. Compared to our early material efforts, also shown in Fig. 9, we see that MAPLE DW is able to deposit low and intermediate  $k$  dielectric elements with close to 1% losses at microwave frequencies. But what is also apparent from Fig. 9 is the current inability of our process to deposit materials with high  $k$  values. The reason our  $k$  values are low is because of our inability to fully densify the starting composite.

An example of the value of optimizing the materials for high density is shown in Fig. 10 where a comparison of the surface SEM micrograph images is made between two different starting compositions. The composition of the dielectric material shown in

(a)

Low Precursor Composition  
 $\epsilon = 50$



(b)

Higher Precursor Composition  
 $\epsilon = 90$

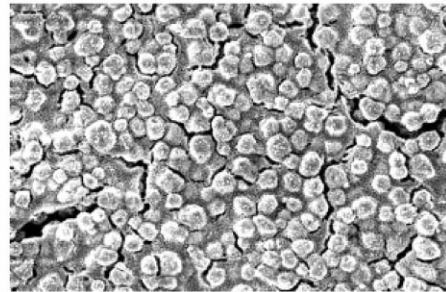


Fig. 10. A comparison of the surface SEM micrograph images made between two different starting compositions of  $\text{BaTiO}_3$  powder and titania precursor.

Fig. 10a does not have as much precursor as compared to Fig. 10b. The comparison shows that by adding an increased amount of dielectric chemical precursor, the air-filled voids can be largely filled. Also obvious from Fig. 10b is the effect of having too much chemical precursor. The thermal decomposition of the chemical precursor to dielectric, in this case titania, occurs with a reduction in size and this results in cracking of the coating. Nevertheless, the dielectric composite in Fig. 10b has almost double the dielectric constant of that for Fig. 10a. Note that the areal density of powder has not changed.

The novelty in the MAPLE DW process is that the interaction of the incident laser pulse with the coating on the ribbon can transfer the micron-size powder, nanopowders and especially the chemical precursors to form a densely packed composite on the receiving substrate. The transfer process must be extremely gentle because it is important for the low decomposition chemical precursors to transfer without reacting. In fact, the MAPLE DW process has been used to transfer whole living cells of *E. Coli* bacteria in patterns with the bacteria remaining viable [11]. The combination of processing biomaterials and electronic materials by a single technique holds great potential for future sensors and interfacing to biological systems.

### 3. Conclusions

We have demonstrated a novel pulsed UV laser direct writing technique called MAPLE DW for the fabrication of conformal electronic devices. MAPLE DW (matrix assisted pulsed laser evaporation direct write) is a soft laser forward transfer technique that takes place in air and at room temperature. Several examples of discrete devices fabricated by MAPLE DW have been given as well as examples of the in situ micro-machining capability. Specific experimental results for the deposition of Ag metal and BaTiO<sub>3</sub>

composite dielectrics with electrical quality comparable to conventional thick film deposition techniques were given and a discussion of the density issue for further electronic device improvement was presented. The mechanism of the MAPLE DW process that makes it applicable to a broad class of electronic materials and even biomaterials has been described.

### Acknowledgements

We gratefully acknowledge the Office of Naval Research and the DARPA MICE Programme for supporting this work.

### References

- [1] A. Piqué, D.B. Chrisey, R.C.Y. Auyeung, J.M. Fitz-Gerald, H.D. Wu, R.A. McGill, S. Lakeou, P.K. Wu, V. Nguyen, M. Duignan, *Appl. Phys. A* 69 (1999) S279–S284.
- [2] D.B. Chrisey, A. Piqué, J.M. Fitz-Gerald, R.C.Y. Auyeung, R.A. McGill, H.D. Wu, M. Duignan, *Appl. Surf. Sci.* 154 (2000) 593–600.
- [3] J.M. Fitz-Gerald, A. Piqué, D.B. Chrisey, P.D. Rack, M. Zeleznik, R.C.Y. Auyeung, S. Lakeou, *Appl. Phys. Lett.* 76 (2000) 1386–1388.
- [4] J. Bohandy, B.F. Kim, F.J. Adrian, *J. Appl. Phys.* 60 (1986) 1538–1539.
- [5] J. Bohandy, B.F. Kim, F.J. Adrian, A.N. Jette, *J. Appl. Phys.* 63 (1988) 1158–1162.
- [6] I. Zergioti, S. Mailis, N.A. Vainos, C. Fotakis, S. Chen, C.P. Grigoropoulos, *Appl. Surf. Sci.* 127–129 (1998) 601–605.
- [7] F.J. Adrian, J. Bohandy, B.F. Kim, A.N. Jette, P. Thompson, *J. Vac. Sci. Tech. B5* (1987) 1490–1494.
- [8] I. Zergioti, S. Mailis, N.A. Vainos, P. Papakonstantinou, C. Kalpouzos, C.P. Grigoropoulos, C. Fotakis, *Appl. Phys. A* 66 (1998) 579–582.
- [9] H. Esrom, J.-Y. Zhang, U. Kogelschatz, A. Pedraza, *Appl. Surf. Sci.* 86 (1995) 202–207.
- [10] S.M. Pimenov, G.A. Shafeev, A.A. Smolin, V.I. Konov, B.K. Bodolaga, *Appl. Surf. Sci.* 86 (1995) 208–212.
- [11] B.R. Ringeisen, D.B. Chrisey, A. Piqué, H.D. Young, R. Modi, M. Bucaro, J. Jones-Meehan, B.J. Spargo, in preparation.